

Thickness dependent structural and magnetic properties of ultra-thin Fe/Al structures

R. Brajpuria^a, S. Tripathi, A. Sharma, T. Shripathi, and S.M. Chaudhari

UGC-DAE Consortium for Scientific Research, University Campus, Khandwa Road, Indore 452 017, India

Received 20 January 2005 / Received in final form 23 December 2005

Published online 31 May 2006 – © EDP Sciences, Società Italiana di Fisica, Springer-Verlag 2006

Abstract. The structural and magnetic properties of electron beam evaporated ultra-thin Fe/Al structures are studied as a function of Fe layer thickness, while keeping the Al layer thickness constant. The grazing incidence X-ray reflectivity measurements carried out on the structures having Fe layer thickness ≤ 20 Å show substantial intermixing between the layers during deposition, indicated by a loss of periodicity. These structures resemble a composite single layer film consisting of Fe and Al clusters. However, for thicker Fe layers (≥ 30 Å), the appearance of a first order Bragg peak in the reflectivity patterns indicates the formation of a better-multilayered structure. These results are also supported by AFM and resistivity measurements. The X-ray diffraction measurements show that in all the multilayer films, deposited Fe layers are textured mainly along (110) direction. The corresponding magnetic measurements show a soft magnetic behaviour of the films with an in-plane easy direction of the magnetization. The observed soft magnetic behaviour in these samples is explained in terms of (i) weak crystalline magnetic anisotropy due to small crystal grains and magnetostriction and (ii) the morphological and structural changes occurring due to the variation in the Fe layer thickness below the critical value in the deposited structures.

PACS. 68.65.Ac Multilayers – 75.70.-i Magnetic properties of thin films, surfaces, and interfaces

1 Introduction

Fe-based soft-magnetic films with a high saturation magnetization and a low coercivity are the most suitable head core materials for high-density magnetic recording. However, Fe thin films deposited by conventional sputtering methods do not exhibit sufficiently low coercivity and high relative permeability due to large magneto crystalline anisotropy, magnetostriction, and internal stress. They could be useful in thin film type magnetic heads if their soft magnetic properties could be significantly improved. It is known that the soft magnetic properties of Fe films can be improved by reducing their grain size by boundary nitridation [1,2] and multilayer (ML) formation [3,4]. In recent years, magnetic multilayered films with artificial periodicity have attracted much attention because they have unusual magnetic properties and show the possibility for applications as new magnetic materials. Among various combinations of elements used to fabricate such multilayered films, much attention has been focused on the combination of the elements with different crystal structure [5–7]. Multilayers, particularly those consisting of pure Fe and non-magnetic layers are expected to have excellent soft magnetic properties because of their high saturation magnetization and

Fe magnetic domain control. Various nonmagnetic layers e.g., Cu, Al₂O₃, C, Si, Ti, SiO₂ and ZnO₂ were incorporated and these ML films show good soft-magnetic properties [4,8–10]. In this respect, Fe/Al bilayer and ML systems have recently also been studied extensively because of their attractive soft magnetic properties such as low coercivity and high saturation magnetization, etc. This makes them good candidates for the possible applications mentioned above [11–16]. However, the fundamental magnetic and electronic properties of these structures are quite different from their bulk counterparts, and over the last decade, it has been shown that these interesting properties are greatly influenced by various micro structural ML parameters such as the individual layer thickness, the number of bilayers and the quality of interfaces formed under different growth conditions [17–25]. In many cases, interdiffusion and reaction phenomena at interfaces can occur during deposition in such ultra thin structures causing a loss of periodicity below a certain thickness, which critically alters the structural and magnetic properties of these MLs. Recently, Carbuicchio et al. have found that with decreasing Fe layer thickness, Al diffusion occurs at the interfaces along preferential paths such as grain boundaries, giving rise to the formation of a solid solution and paramagnetic compounds at the interfaces. They have also found that the magnetic behaviour progressively evolves

^a e-mail: ranjeetbrajpuria@yahoo.com

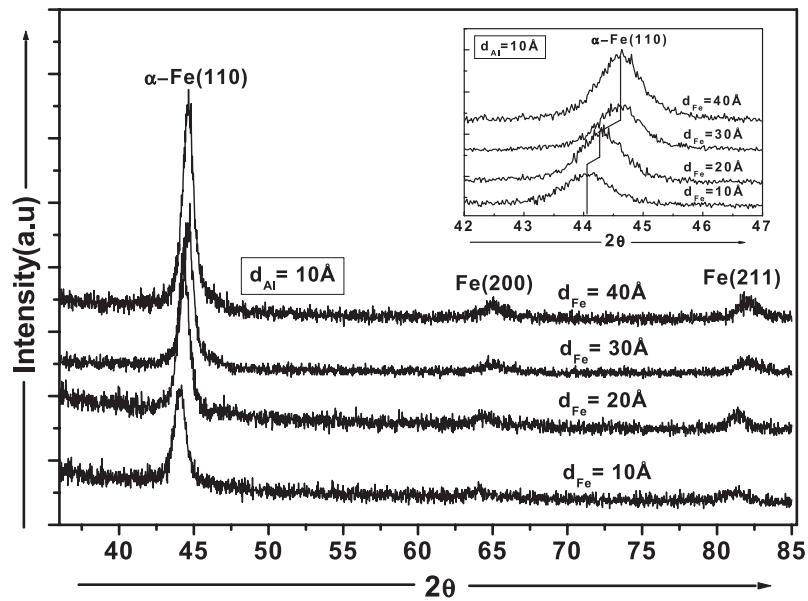


Fig. 1. GIXRD patterns of the as prepared $[\text{Fe} (d_{\text{Fe}})/\text{Al} (10\text{\AA})] \times 15$ MLS.

from ferromagnetic to super-paramagnetic [26,27]. However, the above-mentioned studies lack a discussion of the unusual magnetic behaviour in terms of changes in the microstructural parameters of these structures. In such a situation, one needs a careful characterization of these structures in order to understand the role of the microstructural parameters, and in interpreting the various properties exhibited by them. Therefore, in the present investigation we have systematically carried out the structural and magnetic characterization of bilayers and ML samples using a combination of various non-destructive techniques such as grazing incidence X-ray diffraction (GIXRD), X-ray reflectivity (GIXRR), atomic force microscopy (AFM), four-probe resistivity and vibrating sample magnetometer (VSM), in order to extract a clear correlation between the structural parameters and observed magnetization behaviour in Fe/Al ML samples.

2 Experimental details

In the present work, a set of ML samples, each with 15 bilayers, was prepared with a constant Al thickness of 10 Å and a Fe layer thickness varying from 10 Å to 40 Å in steps of 10 Å, respectively, on float glass substrates, using an e-beam evaporation system [28] under UHV ($\sim 8 \times 10^{-9}$ Torr) conditions at room temperature. The deposition rate of 0.1 Å/s for both Fe and Al was controlled using a quartz crystal thickness monitor. A capping layer of 20 Å of Al was deposited on the top of each sample in order to protect the MLs from oxidation. The first layer on the substrate was of Al. The substrates were placed symmetrically at a vertical distance of 60 cm from both sources in order to assure a uniform thickness of the deposition on the substrates. All the ML samples with the various Fe layer thicknesses were deposited in a single run

without breaking the vacuum by using a substrate masking facility.

The micro-structural and morphological investigations of the MLs were carried out using GIXRD, GIXRR and AFM techniques. The GIXRD and GIXRR measurements were done using a Siemens D5000 diffractometer equipped with a sealed Cu tube as the source of X-rays at $\lambda = 1.542$ Å, operated at 40 KV and 30 mA. All the GIXRD patterns were recorded at an incidence angle of 0.5° . AFM measurements were carried out using a DI Nanoscope-III AFM set-up in contact mode. The corresponding magnetic and transport properties were measured at room temperature using the VSM and four probe resistivity techniques.

3 Results and discussion

A single characterization technique provides only incomplete information on the various micro-structural aspects involved in a multilayer structure (MLS). In order to get more clear and understandable picture of the deposited MLS, we have, therefore, used different non-destructive techniques and the corresponding results are presented in the following sections.

3.1 Grazing incidence X-ray diffraction measurements

Figure 1 shows the GIXRD patterns for an as prepared $[\text{Fe} (d_{\text{Fe}})/\text{Al} (10\text{\AA})] \times 15$ MLS. From the recorded diffraction curves, it is clearly seen that all the deposited MLS are textured mainly along (110) direction of α -Fe. The other two low intensity peaks are due to the reflections from the Fe (200) and Fe (220) planes. The peaks corresponding to Al were not detected in any of the recorded spectrums, indicating that the deposited ultra thin Al

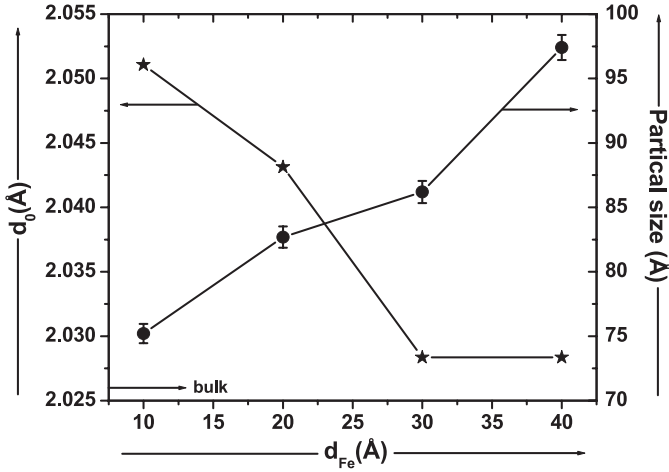


Fig. 2. Dependence of the average spacing ' d ' and particle size on the Fe layer thickness.

layer is amorphous in nature. At a greater Fe layer thickness, the peak due to α -Fe at $2\theta = 44.62^\circ$ matches well with that of bulk Fe (44.67°) [29]. However, at lower d_{Fe} , it is found that the peak is broadened and shifted towards a lower 2θ (44.1°) value (shown in the inset of Fig. 1). This may be due to substantial intermixing between Fe and Al layers at the interface occurring during the deposition, leading to a distorted Fe lattice structure. The corresponding particle sizes of Fe as determined from measured GIXRD patterns using the Scherrer formula are shown in Figure 2. It is observed that the average particle size increases monotonically with increasing d_{Fe} . In addition to this, we have also measured the d spacing of α -Fe crystallites in these MLS as a function of d_{Fe} (shown in the same Fig. 2). It is found that the d spacing decreases from 2.052 Å to 2.028 Å as the Fe layer thickness increases and this matches fairly well with bulk d spacing ($d = 2.026$ Å) at $d_{Fe} = 40$ Å. The variation in the d spacing as a function of d_{Fe} indicates the presence of stresses in the deposited layers. At lower Fe thicknesses it suggests a compressive stress, which is released as d_{Fe} increases to form a continuous layer.

3.2 Grazing incidence X-ray reflectivity measurements

A better understanding of the micro-structural parameters of these MLS can be obtained by a careful analysis of the recorded GIXRR patterns. The GIXRR patterns reported in Figure 3 corresponding to [Fe (10 Å)/Al (10 Å)] $\times 15$ and [Fe (20 Å)/Al (10 Å)] $\times 15$ ML samples do not look like typical patterns of a MLS. One would expect to observe well defined Bragg-like peaks due to the periodicity of the ML, suggesting a large amount of intermixing at the interface during deposition. Indeed this is expected because the Al and Fe thicknesses involved in these samples are very small and may not form continuous layers that would lead to well defined interfaces. This

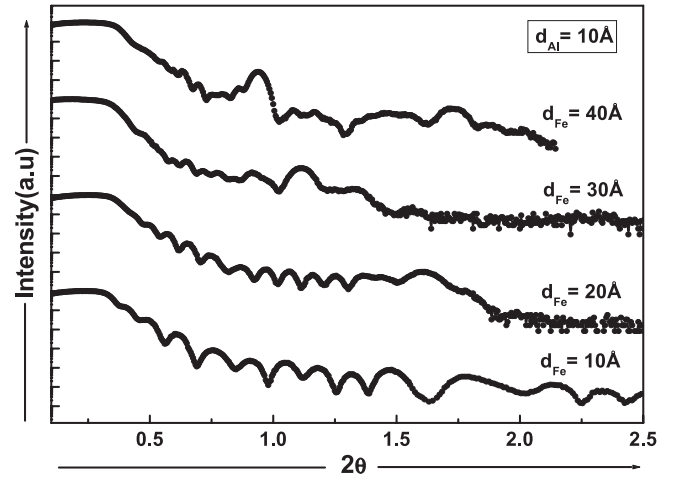


Fig. 3. GIXRR patterns of the as prepared [Fe (d_{Fe})/Al (10 Å)] $\times 15$ MLS.

is revealed by our GIXRD results. The deposited structures in both cases show a single mixed layer consisting of Fe and Al clusters. Whereas at greater Fe layer thicknesses of 30 Å and 40 Å, the deposited structures show the clear appearance of first order Bragg reflection, indicating the formation of a better layered structure. The calculated modulation wavelengths of 38.5 Å and 47.3 Å match fairly well with the nominal bilayer periodicity. The total thickness calculated for the lower periodicity samples also matches well with the deposited layer thickness when they are considered as a composite single layer in both cases.

3.3 AFM measurements

More clear information about the structure and surface morphology can be obtained from AFM studies conducted on Fe/Al bilayer samples prepared under similar conditions as that of ML samples. Figure 4 shows the three-dimensional AFM images for [Fe (d_{Fe})/Al (10 Å)] bilayer samples obtained from a $1 \times 1 \mu\text{m}^2$ sample area using contact mode. It is clearly seen from Figures 4a and 4b that deposited layers are nearly continuous in the case of [Fe (10 Å)/Al (10 Å)] and [Fe (20 Å)/Al (10 Å)] bilayer samples. This suggests an island type growth, where Fe clusters are embedded in an Al matrix, giving rise to a very large surface roughness value. Figure 5 shows the variation in surface roughness as a function of d_{Fe} . It is clear from the figure that as the thickness of the Fe layer increases, the value of the surface roughness increases and is found to be a maximum for $d_{Fe} = 20$ Å (22.9 Å). So one can understand from the obtained reflectivity patterns and from the above AFM images, why a well-defined MLS is not observed for lower Fe layer thicknesses. As the Fe layer thickness is increased further to ≥ 30 Å, the AFM images show the formation of more continuous and denser layers compared to the above-mentioned cases and as a result the

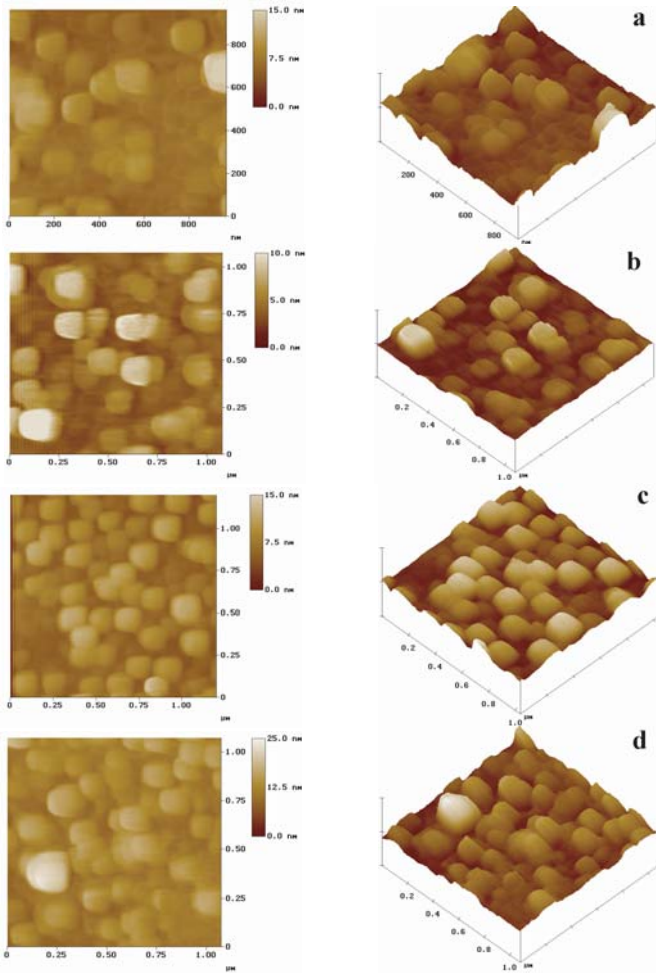


Fig. 4. Two and three-dimensional AFM images of (a) [Fe (10 Å)/Al (10 Å)], (b) [Fe (20 Å)/Al (10 Å)], (c) [Fe (30 Å)/Al (10 Å)] and (d) [Fe (40 Å)/Al (10 Å)] bilayer samples.

value of the surface roughness decreases to 16.2 Å. This is in correlation with the reflectivity patterns. Hence, the obtained AFM pictures provide us with clearer information about the different growth stages, as the Fe layer thickness is increased from 10 Å to 40 Å. These results obtained from the AFM study along with the other structural investigations help in interpreting the observed resistivity and magnetization behaviour.

3.4 Resistivity measurements

Figure 6 shows the dependence of the resistivity as a function of d_{Fe} in Fe/Al MLS. The resistivity of the MLS decreases rapidly with increasing Fe layer thickness. This dependence is similar to the thickness dependence of a metallic single layered film [8]. Thus, it is possible to deduce the structure of each layer in the deposited ML samples from the resistivity measurements. It is seen that for a lower d_{Fe} , the resistivity is a maximum (127.1 $\mu\Omega$ cm), suggesting that the deposited layers are far away from the percolation threshold. The AFM measurements indeed confirm

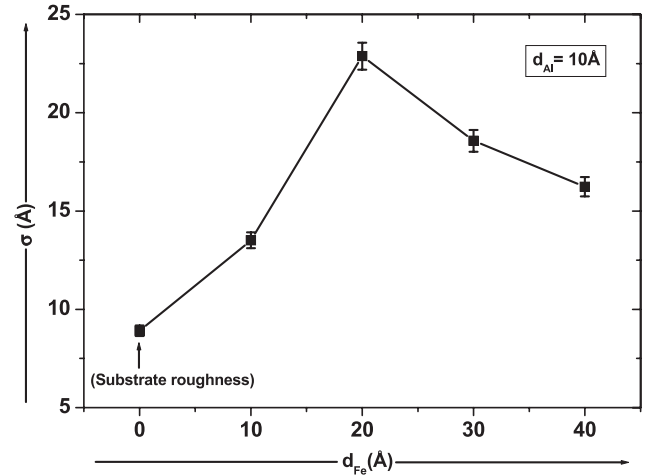


Fig. 5. Variation in the surface roughness as a function of the Fe layer thickness.

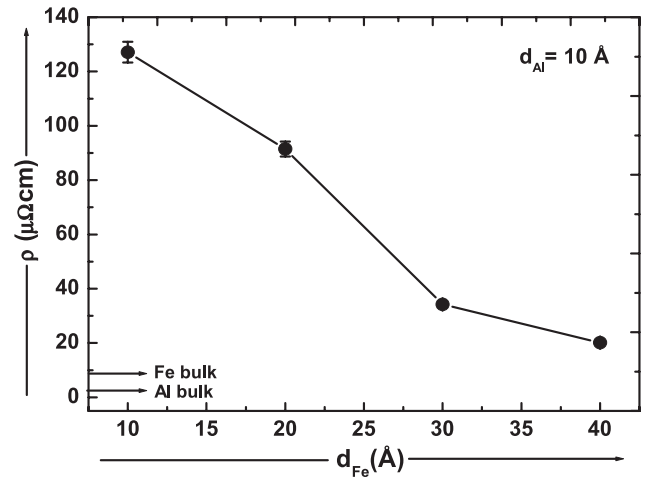


Fig. 6. Dependence of the resistivity on the Fe layer thickness.

the above statement as discussed earlier. As the Fe thickness increases to 30 Å and 40 Å, the resistivity drops to a minimum indicating the formation of more continuous layers.

3.5 Magnetic measurements

The magnetization measurements reported in the present study were carried out using a low field vibrating sample magnetometer. In all the measurements, the magnetic field was applied parallel to the surface of the film plane and hysteresis loops were recorded up to the saturation of the magnetization.

Figure 7 shows the M-H loops measured at room temperature for Fe/Al MLS having different d_{Fe} . The corresponding coercivity (H_c), saturation field (H_s) and magnetization (M_s) values determined from the above hysteresis loops are plotted in Figure 8. It should be noted that the entire ML samples show a saturation of the magnetization with applied magnetic field suggesting an in-plane easy direction of the magnetization. Figures 7a and 7b

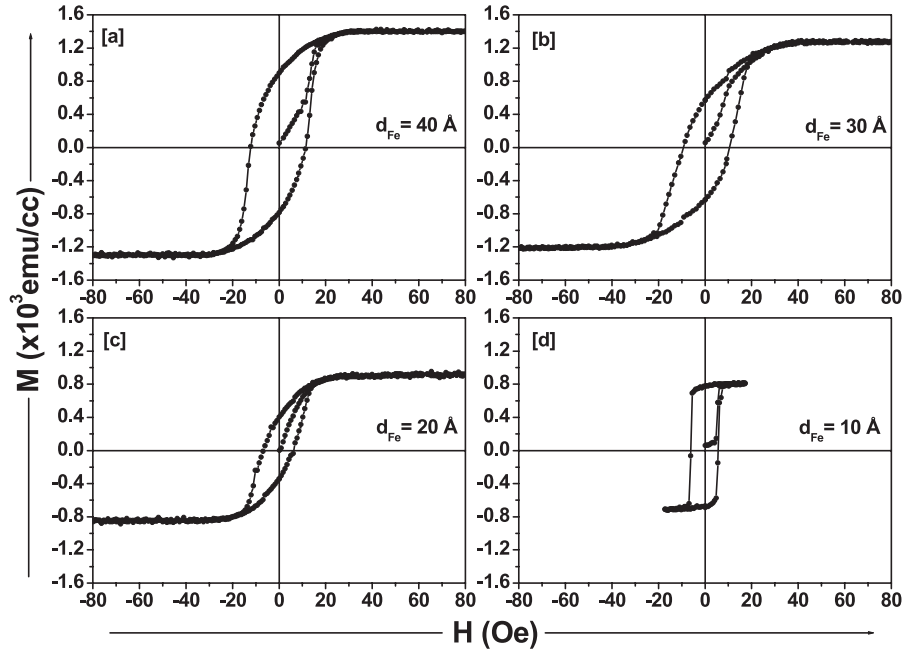


Fig. 7. Hysteresis loops for the as prepared (a) [Fe (40 Å)/Al (10 Å)] $\times 15$, (b) [Fe (30 Å)/Al (10 Å)] $\times 15$, (c) [Fe (20 Å)/Al (10 Å)] $\times 15$, and (d) [Fe (10 Å)/Al (10 Å)] $\times 15$ MLS.

shows hysteresis loops corresponding to [Fe (40 Å)/Al (10 Å)] $\times 15$ and [Fe (30 Å)/Al (10 Å)] $\times 15$ MLS. From the nature of the hysteresis loops, it is clear that the obtained magnetization behaviour is mainly due to the gradual response of the domain walls and domain motion in the ferromagnetic Fe layers under the applied magnetic field. From the recorded hysteresis loops, the estimated H_c , H_s and M_s values are found to be 10.7 Oe, 30.2 Oe, 1.35×10^3 emu/cc for the [Fe (40 Å)/Al (10 Å)] $\times 15$ and 8.15 Oe, 39.8 Oe, 1.23×10^3 emu/cc for the [Fe (30 Å)/Al (10 Å)] $\times 15$ MLS, respectively. The small values of coercivity and saturation field indicate a soft magnetic nature of the MLS and can be explained by the weak crystalline magnetic anisotropy due to the existence of small crystal grains and negligible magnetostriction. Additionally, it has been reported in the literature that the domain wall energy, in MLS consisting of magnetic and nonmagnetic layers, becomes smaller than that of the single layer film [30]. Therefore, the decrease of the domain wall energy due to the magnetostatic coupling between Fe layers could be an additional way to improve the soft magnetic properties. Similar results are also reported by Senda et al. in their investigation carried out on MLS consisting of Fe and nonmagnetic layers of Al₂O₃, Cu, C, Si and Ti prepared with the sputtering technique [4]. However, the M_s values obtained for these MLS are much lower than that of the bulk Fe (1.732×10^3 emu/cc), suggesting the formation of a nonmagnetic FeAl intermetallic layer at the interface, which is also reflected from structural studies.

Figures 7c and 7d shows the hysteresis loops recorded on ML samples having a Fe layer thickness of 20 Å and 10 Å, respectively. It can be seen from Figure 8 that the values of H_c , H_s and M_s are drastically reduced as the Fe layer thickness decreases and show a minimum

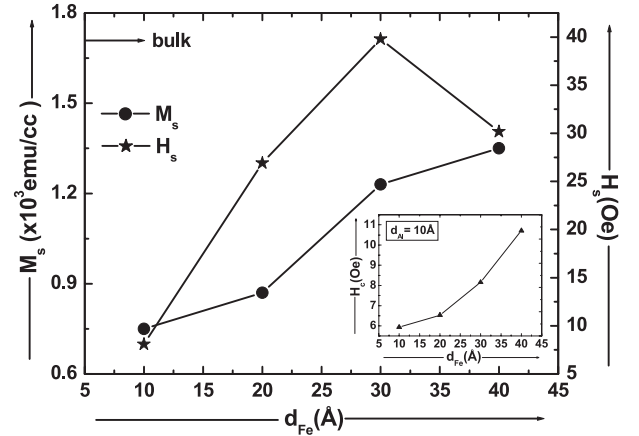


Fig. 8. Dependence of the H_c , H_s and M_s values on the Fe layer thickness.

($H_c = 5.9$ Oe, $H_s = 8.1$ Oe and $M_s = 0.75 \times 10^3$ emu/cc) for the $d_{Fe} = 10$ Å MLS. The observed drastic changes in the hysteresis loop at this thickness can be better explained as follows: (i) as Fe layer thickness is reduced below a critical value the deposited structure does not form a MLS at all and the resulting deposited MLS, as indicated by the structural studies, resembles a composite single layer film consisting of Fe and Al nano size clusters; (ii) the decrease of the grain size and pure ferromagnetic Fe content corresponds to an increase of the surrounding paramagnetic compounds at the interfaces. Thus, the observed magnetization behaviour in the present case mainly reflects the super-paramagnetic nature of the sample. Similar behaviour is also obtained and reported by Kumar et al. [31] and Carbuicchio et al. [26]. They found that,

below a particular thickness, the samples change from ferromagnetic to super-paramagnetic. Hence all these measurements lead to the conclusion that the observed magnetization behaviour for $[\text{Fe} (10 \text{ \AA})/\text{Al} (10 \text{ \AA})] \times 15$ MLS is due to the super paramagnetic nature of nano sized Fe clusters embedded in an Al matrix.

4 Conclusions

The effects of the Fe layer thickness on the structural, magnetic and transport properties in ultrathin Fe/Al MLS have been investigated using GIXRD, GIXRR, AFM, resistivity and VSM measurements. The structural and morphological measurements carried out on these MLS show substantial intermixing and the deposited structure resembles a composite single layer film consisting of Fe and Al clusters at lower Fe layer thicknesses. The observed soft magnetic behaviour of the ML samples is attributed to a weak crystalline magnetic anisotropy due to the existence of small crystal grains and magnetostriiction. However, at lower Fe layer thicknesses, the observed behaviour is mainly due to the formation of super-paramagnetic nano-sized Fe clusters embedded in an Al matrix.

The authors would like to thank Prof. R.K. Pandey and Dr. V. Ganeshan for the GIXRD and AFM measurements. Special thanks are due for the help rendered by Mr. S. Potdar and Mr. A. Wadiker for depositing the ML samples. This work is dedicated to the memory of Dr. S.M. Chaudhari who untimely passed away during this work.

References

- O. Shimizu, K. Nakanishi, S. Yoshida, *J. Appl. Phys.* **70**, 6244 (1991)
- N. Terada, Y. Hoshi, M. Naoe, S. Yamanaka, *IEEE Trans. Magn. Mag.* **20**, 1451 (1984)
- T. Kobayashi, R. Nkatani, S. Ootomo, N. Kumasaka, *J. Appl. Phys.* **64**, 3157 (1989)
- M. Senda, Y. Nagai, *J. Appl. Phys.* **65**, 3157 (1989)
- H. Grimmer, P. Böni, U. Breirmeier, D. Clemens, M. Horisberger, H.C. Mertins, F. Schäfers, *Thin Solid Films* **319**, 73 (1998)
- L.N. Tong, M.H. Pan, J. Wu, X.S. Wu, J. Du, M. Lu, D. Feng, H.R. Zhai, H. Xia, *Eur. Phys. J. B* **5**, 61 (1998)
- P. Gruenberg, R. Schreiber, Y. Pang, M.B. Brodsky, H. Sowers, *Phys. Rev. Lett.* **57**, 2442 (1986)
- Y. Kozono, M. Komuro, S. Narishige, M. Hanazaono, Y. Sugita, *J. Appl. Phys.* **61**, 4311 (1987)
- M. Senda, Y. Nagai, *J. Appl. Phys.* **65**, 3151 (1989)
- T. Miyazaki, F. Sato, *J. Magn. Magn. Mater.* **78**, 40 (1989)
- F. D'Orazio, G. Gubbiotti, F. Lucari, E. Tassoni, *J. Magn. Magn. Mater* **242**, 535 (2002)
- G.V. Sudhakar Rao, A.K. Bhatnagar, F.S. Razavi, *J. Magn. Magn. Mater* **247**, 159 (2002)
- N. Tezuka, M. Oogane, T. Miyazaki, *J. Magn. Magn. Mater.* **198**, 149 (1999)
- H. Chen, Q.Y. Xu, G. Ni, J. Lu, H. Sang, S.Y. Zhang, Y.W. Du, *J. Appl. Phys.* **85**, 5798 (1999)
- T. Hamaguchi, H. Aida, S. Nakagawa, M. Naoe, *J. Appl. Phys.* **73**, 6444 (1993)
- T. Haeiwa, H. Negoro, M. Matsumoto, *J. Appl. Phys.* **69**, 5346 (1991)
- F. Albertini, G. Carlotti, F. Carlotti, F. Casoli, G. Gubbiotti, H. Koo, R.D. Gamez, *J. Magn. Magn. Mater.* **240**, 526 (2002)
- R. Allenspach, M. stampanoni, A. Bischof, *Phys. Rev. Lett.* **65**, 3344 (1990)
- C.H. Lee, H. He, F.J. Lameelas, W. Vavra, C. Uher, R. Clarke, *Phys. Rev. B* **42**, 1066 (1990)
- E. Fonda, A. Traverse, *J. Magn. Magn. Mater.* **268**, 292 (2004)
- P. Bhattacharya, K.N. Ishihara, K. Chattopadhyay, *Mater. Sci. Eng. A* **304**, 250 (2001)
- M. Carbucicchio, M. Rateo, G. Ruggiero, G. Turilli, *Hyperfine Inter.* **113**, 303 (1998)
- T. Geilman, J. Chevallier, M. Fanciulli, G. Weyer, V. Nevolin, A. Zenkevitch, *Appl. Surf. Sci.* **109**, 570 (1997)
- A.R. Chowdhury, A.E. Freitag, *J. Appl. Phys.* **79**, 6303 (1996)
- O. Lenoble, Ph. Bauer, J.F. Bobo, H. Fisher, M.F. Ravet, M. Piccuch, *J. Phys. Condens. Matter.* **6**, 3337 (1994)
- M. Carbucicchio, C. Grazzi, M. Rateo, G. Ruggiero, M. Solzi, G. Turilli, *J. Magn. Magn. Mater.* **215**, 563 (2000)
- M. Carbucicchio, M. Rateo, G. Ruggiero, M. Solzi, G. Turilli, *J. Magn. Magn. Mater.* **196**, 33 (1999)
- S.M. Chaudhari, N. Suresh, D.M. Phase, A. Gupta, B.A. Dasannacharya, *J. Vac. Sci. Tech. A* **17**, 242 (1999)
- JCPDS file Nos. 4-787 and 6-696
- A. Yelon, in *Physics of Thin films* edited by M.H. Francombe, R.W. Hoffman (Academic Press, New York, 1971), Vol. 6
- D. Kumar, J. Narayan, A.V. Kavita, A.K. Sharma, J. Sankar, *J. Magn. Magn. Mater.* **232**, 161 (2001)